CAPACITY OF PPM ON APD-DETECTED OPTICAL CHANNELS

S. Dolinar, D. Divsalar, J. Hamkins, F. Pollara
Jet Propulsion Laboratory, California Institute of Technology, Pasadena, CA
e-mail: {sam,dariush,hamkins,fabrizio}@shannon.jpl.nasa.gov

ABSTRACT

This report defines the fundamental parameters affecting the capacity of a soft-decision optical channel, and relates them to corresponding parameters for the well-understood AWGN channel. For example, just as the performance on a standard additive white Gaussian noise (AWGN) channel is fully characterized by its SNR, a corresponding Webb channel is fully characterized by its SNR, and a single additional skewness parameter δ^2 which depends on the photon detector. In fact, this Webb channel reduces to the standard AWGN channel when $\delta^2 \to \infty$.

Numerical results show that the capacity of M-ary orthogonal signaling on the Webb channel exhibits the same brick-wall Shannon limit $(M \ln 2)/(M-1)$ as on the AWGN channel (≈ -1.59 dB for large M), and that soft output channels offer a 3 dB advantage over hard output channels.

I. INTRODUCTION

In an optical communication system using M-ary pulse position modulation (PPM), the probability density function describing the number q of photons at the output of an avalanche photodiode detector is accurately approximated by [2]:

$$p(q) = \frac{1}{\sqrt{2\pi\bar{n}G^2F}}\left(1+\frac{(q-G\bar{n})(F-1)}{GF\bar{n}}\right)^{-3/2} \cdot \exp\left(-\frac{(q-G\bar{n})^2}{2\bar{n}G^2F\left(1+\frac{(q-G\bar{n})(F-1)}{GF\bar{n}}\right)}\right), \quad q > \frac{-G\bar{n}}{F-1} \tag{1}$$

where $\bar{n}$ is the mean number of photons absorbed by the APD, G is the APD gain, and $F = k_{eff}G + (2 - 1/G)(1 - k_{eff})$ is an excess noise factor. The Webb model for PPM signaling (here called Webb-2) uses the density in Eq. (1) twice: once using the average number $\bar{n}_1$ of photons in the signal slot, and a second time using the average number $\bar{n}_0$ of photons in the $M-1$ non-signal slots.

The Webb-distributed electron count q is conveniently represented in terms of a standardized (scaled-and-translated) Webb random variable w. Defining $q = m + w\sigma$, where $m = G\bar{n}$ and $\sigma = \sqrt{\bar{n}G^2F}$, the probability density for the standardized Webb random variable w simplifies to

$$p(w;\delta^2) = \frac{1}{\sqrt{2\pi}}(1+w/\delta)^{-3/2}e^{-w^2/2(1+w/\delta)}, \quad w > -\delta \tag{2}$$

where $\delta^2 = \bar{n}F/(F-1)^2$. Note that this standardized Webb probability reduces exactly to a standardized Gaussian when the parameter $\delta^2 \to \infty$.

If w is a standardized Webb random variable with skewness parameter δ^2 and probability density given by Eq. (2), then $q = m + w\sigma$ is a Webb random variable with mean m, variance σ^2, and skewness δ^2, and is denoted as $W(m, \sigma^2, \delta^2)$. The standardized Webb random variable has zero mean, unit variance and can be denoted $w = W(0, 1, \delta^2)$.

Our objective in this paper is to develop an understanding of the role of various optical parameters on the capacity of an optical communication system, and to this end we compute and compare the capacities of various idealized channels which might be used to approximate the optical communication channel. We also compare the capacities achievable with soft- and hard-decision channel outputs.

II. CAPACITY OF PPM ON CHANNELS WITH SOFT OUTPUTS

For each channel model we consider the communication system shown in Fig. 1. The output $\mathbf{U} = (U_1, U_2, \ldots, U_k)$ of a k-bit source is modulated with $(M = 2^k)$-ary PPM to yield a signal $\mathbf{X} = (X_1, X_2, \ldots, X_M)$. The capacity of M-PPM is the same as that of an orthogonal signal set with M codewords, and of M-FSK.

The capacity of PPM modulation on the channel is the maximum amount of information that can be transmitted reliably and is given by $C = \max_{\mathbf{p}(\mathbf{X})} I(\mathbf{Y};\mathbf{X})$.

This work was funded by the TMOD Technology Program and performed at the Jet Propulsion Laboratory, California Institute of Technology under contract with the National Aeronautics and Space Administration.

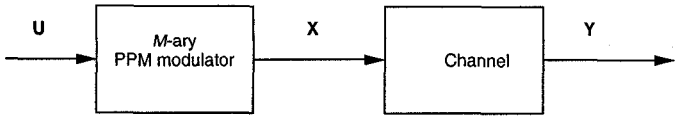

Fig. 1. Model of PPM signaling.

The channel capacity with input signals restricted to an M-ary orthogonal constellation $\mathcal{C}$, and no restriction on the channel output, is given by

$$C = \sum_{\mathbf{x}\in\mathcal{C}} \int_{\mathbf{y}} \frac{1}{M} p(\mathbf{y}|\mathbf{x}) \log_2 \left(\frac{p(\mathbf{y}|\mathbf{x})}{\frac{1}{M}\sum_{\hat{\mathbf{x}}\in\mathcal{C}} p(\mathbf{y}|\hat{\mathbf{x}})} \right) d\mathbf{y}, \quad (3)$$

where $\mathbf{y} = (y_1, \ldots, y_M)$ is the received vector. Because of the symmetry of orthogonal signals and of the channels considered, capacity is achieved with an equiprobable M-ary source distribution, and Eq. (3) reduces to

$$C = \log_2 M - E_{\mathbf{v}|\mathbf{x}_1} \log_2 \left[\frac{\sum_{j=1}^{M} p(\mathbf{v}|\mathbf{x}_j)}{p(\mathbf{v}|\mathbf{x}_1)} \right] \quad (4)$$

where $\mathbf{v}$ is a random vector obtained from $\mathbf{y}$ via an arbitrary invertible transformation. Uninspired computation of the expectation of the right side of Eq. (4) requires evaluation of an M-dimensional integral. Alternatively, this M-dimensional expectation can be accurately estimated via Monte Carlo simulation, at much lower complexity.

A. Capacity of M-ary PPM on the Standard AWGN Channel (AWGN-1)

In this case, the possible signals $\mathbf{X}$ are of the form $\mathbf{x}_j = (x_{j1}, \ldots, x_{jM}) = (0, 0, 0, \ldots, m, 0, \ldots, 0)$ where the nonzero signal value m is in position j. The transmitted vector $\mathbf{x}$ is corrupted by additive white Gaussian noise with zero mean and variance σ^2 in each component:

$$\begin{cases} y_j & \text{is } N(m, \sigma^2) & \text{(signal present)} \\ y_i & \text{is } N(0, \sigma^2), \quad i \neq j & \text{(signal absent)} \end{cases} \quad (5)$$

This is the model for any set of M-ary orthogonal signals, with energy per M-dimensional symbol $E_s = m^2$, transmitted on an AWGN channel with two-sided noise spectral density $N_0/2 = \sigma^2$. A symbol signal-to-noise ratio (SNR) can be defined by $\rho = m^2/\sigma^2 = 2E_s/N_0$.

For the distributions in Eq. (5), we have

$$p(\mathbf{y}|\mathbf{x}_j) = \sigma^{-M} \phi\left(\frac{y_j - m}{\sigma}\right) \prod_{\substack{i=1 \\ i\neq j}}^{M} \phi\left(\frac{y_i}{\sigma}\right), \quad (6)$$

where $\phi(x) = \frac{1}{\sqrt{2\pi}} e^{-x^2/2}$. Defining $v_j = y_j/\sigma$, we obtain

$$\frac{p(\mathbf{v}|\mathbf{x}_j)}{p(\mathbf{v}|\mathbf{x}_1)} = e^{(v_j^2 - (v_j - \sqrt{\rho})^2 - v_1^2 + (v_1 - \sqrt{\rho})^2)/2} \quad (7)$$

Using Eq. (7) in Eq. (4) we get an expression for the capacity of orthogonal signaling on the AWGN-1 channel

$$C(\rho) = \log_2 M - E_{\mathbf{v}|\mathbf{x}_1} \log_2 \sum_{j=1}^{M} \exp\left[\sqrt{\rho}(v_j - v_1)\right] \quad (8)$$

B. Capacity of M-ary PPM on a More General Gaussian Channel (AWGN-2)

Now we extend the analysis to cover a "double Gaussian" problem (here called AWGN-2), related more directly to the PPM optical model and characterized by different means and variances depending on whether the signal is present or absent:

$$\begin{cases} y_i & \text{is } N(m_0, \sigma_0^2), \ i \neq j & \text{(signal absent)} \\ y_j & \text{is } N(m_1, \sigma_1^2) & \text{(signal present)}, \end{cases} \quad (9)$$

where $m_1 > m_0$ and $\sigma_1^2 > \sigma_0^2$. By symmetry of the orthogonal PPM signal constellation, capacity can be evaluated by Eq. (4). By straightforward algebra, it follows that

$$\frac{p(\mathbf{y}|\mathbf{x}_j)}{p(\mathbf{y}|\mathbf{x}_1)} = \exp\left[(v_j^2 - u_j^2 - v_1^2 + u_1^2)/2\right] \quad (10)$$

where $v_j = (y_j - m_0)/\sigma_0$ and $u_j = (y_j - m_1)/\sigma_1$. Define $\gamma = \sigma_0^2/\sigma_1^2$ and $\rho = (m_1 - m_0)^2/\sigma_0^2$. Then, given $\mathbf{x}_1$, the $\{v_j\}$ are independent and distributed as

$$\begin{cases} v_1 & \text{is} \quad N(\sqrt{\rho}, 1/\gamma) \\ v_j & \text{is} \quad N(0, 1), \quad j \neq 1. \end{cases} \quad (11)$$

In terms of the $\{v_j\}$, the $\{u_j\}$ are determined by the invertible transformation $u_j = \sqrt{\gamma}(v_j - \sqrt{\rho})$. Thus, we have $u_j \pm v_j = v_j(\sqrt{\gamma} \pm 1) - \sqrt{\gamma\rho}$. Plugging into Eq. (4), we obtain

$$C(\rho, \gamma) = \log_2 M - E_{\mathbf{v}|\mathbf{x}_1} \log_2 \sum_{j=1}^{M} \exp\left[\gamma\sqrt{\rho}(v_j - v_1) + (1-\gamma)(v_j^2 - v_1^2)/2\right]. \quad (12)$$

Note that this equation reduces to the standard AWGN-1 capacity for orthogonal signals (Eq. (8)), when $\gamma \to 1$.

C. Capacity of M-ary PPM on Webb-distributed Channels (Webb-1 and Webb-2)

The Webb-1 channel model simply substitutes Webb random variables W(·,·,·) for the Gaussian random variables N(·,·) in Eq. (5) for the AWGN-1 channel model:

$$\begin{cases} y_j & \text{is } W(m,\sigma^2,\delta^2) & \text{(signal present)} \\ y_i & \text{is } W(0,\sigma^2,\delta^2),\ i \neq j & \text{(signal absent)} \end{cases} \tag{13}$$

The conditional probability density functions are

$$\begin{aligned} p(y_j|\mathbf{x}_j) &= \frac{1}{\sigma} p\left(\frac{y_j - m}{\sigma}; \delta^2\right) \\ p(y_i|\mathbf{x}_j) &= \frac{1}{\sigma} p\left(\frac{y_i}{\sigma}; \delta^2\right), i \neq j, \end{aligned}$$

where $p(\cdot;\cdot)$ is given in Eq. (2). Thus, for the Webb-1 model,

$$\frac{p(\mathbf{y}|\mathbf{x}_j)}{p(\mathbf{y}|\mathbf{x}_1)} = \frac{p(v_j - \sqrt{\rho}; \delta^2)p(v_1;\delta^2)}{p(v_1 - \sqrt{\rho}; \delta^2)p(v_j;\delta^2)}, \tag{14}$$

where, as in the AWGN-1 channel, $v_j = y_j/\sigma$ and $\rho = m^2/\sigma^2$. The capacity of the Webb-1 channel is given by plugging into Eq. (4):

$$C(\rho,\delta) = \log_2 M - E_{\mathbf{v}|\mathbf{x}_1} \log_2 \sum_{j=1}^{M} \frac{p(v_j - \sqrt{\rho}; \delta^2)p(v_1;\delta^2)}{p(v_1 - \sqrt{\rho}; \delta^2)p(v_j;\delta^2)}. \tag{15}$$

The Webb-2 channel model substitutes Webb random variables W(·,·,·) for the Gaussian random variables N(·,·) in Eq. (9) for the AWGN-2 channel model:

$$\begin{cases} y_j & \text{is } W(m_1,\sigma_1^2,\delta_1^2) & \text{(signal present)} \\ y_i & \text{is } W(m_0,\sigma_0^2,\delta_0^2), i \neq j & \text{(signal absent)} \end{cases} \tag{16}$$

Following the same method as in Eq. (14), we have

$$\frac{p(\mathbf{y}|\mathbf{x}_j)}{p(\mathbf{y}|\mathbf{x}_1)} = \frac{p(\sqrt{\gamma}(v_j - \sqrt{\rho}); \delta_1^2)p(v_1;\delta_0^2)}{p(\sqrt{\gamma}(v_1 - \sqrt{\rho}); \delta_1^2)p(v_j;\delta_0^2)}, \tag{17}$$

where, as in the AWGN-2 channel, $v_j = (y_j - m_0)/\sigma_0$, $\gamma = \sigma_0^2/\sigma_1^2$ and $\rho = (m_1 - m_0)^2/\sigma_0^2$. The APD channel imposes an additional constraint that $\sigma_0^2/\sigma_1^2 = \delta_0^2/\delta_1^2$. Using this constraint and defining $\Delta = \delta_1^2 - \delta_0^2$, the capacity of the Webb-2 channel is given by plugging into Eq. (4):

$$\begin{aligned} C(\rho,\gamma,\Delta) &= \log_2 M \\ &- E_{\mathbf{v}|\mathbf{x}_1} \log_2 \sum_{j=1}^{M} \frac{p(\sqrt{\gamma}(v_j - \sqrt{\rho}); \frac{\Delta}{1-\gamma})\ p(v_1; \frac{\gamma\Delta}{1-\gamma})}{p(\sqrt{\gamma}(v_1 - \sqrt{\rho}); \frac{\Delta}{1-\gamma})\ p(v_j; \frac{\gamma\Delta}{1-\gamma})}. \end{aligned} \tag{18}$$

III. CAPACITY AS A FUNCTION OF BIT-SNR

In the case of the classic AWGN-1 channel, the capacity formulas imply a well-known threshold on the minimum required signal-to-noise ratio (SNR) *per information bit* communicated over the channel. If the AWGN-1 *channel-SNR* is E_s/N_0 (per channel symbol), the corresponding *bit-SNR* is computed as $E_b/N_0 = (E_s/N_0)/R$ (per information bit), where R (information bits/channel symbol) is the rate of the overall code applied to the channel. If the rate is at the capacity limit, then $R = C$, and the formula for the minimum possible bit-SNR is $(E_b/N_0)_{\min} = (E_s/N_0)/C$.

To unify the treatment of each channel, we define a minimum bit-SNR parameter $\rho_b = \rho/(2C)$. Note that this definition for the AWGN-1 channel reduces to $\rho_b = (E_s/N_0)/C = (E_b/N_0)_{\min}$.

A. The AWGN-1 Channel

Fig. 2 shows the AWGN-1 capacity as a function of the minimum required bit-SNR $\rho_b = E_b/N_0$. It also shows the E_b/N_0 required for uncoded M-PPM to achieve bit error probability $P_b = 10^{-6}$, where $P_b = \frac{1}{2}\frac{M}{M-1}P_M$, and the probability of uncoded symbol error is

$$P_M = 1 - \int_{-\infty}^{\infty} \phi\left(x - \sqrt{\rho}\right) \Phi(x)^{M-1} dx \tag{19}$$

where $\Phi(x) = \int_{-\infty}^{x} \phi(u)du$. Fig. 2 illustrates the possible improvements to be gained by using coding on M-PPM. This figure also shows, for each M, the capacity limitation imposed by restricting the M-dimensional signaling set to be the orthogonal set. The exact computation of C for larger dimensions is extremely complex and it is necessary to resort to Monte Carlo methods as described in [5, Appendix I].

For M-PPM on an AWGN-1 channel, both the uncoded probability of symbol error and the capacity in Eq. (8) are functions of the single parameter $\rho = m^2/\sigma^2$. This is a statement of the well-known fact that the AWGN-1 channel is fully characterized by its SNR.

B. The AWGN-2 Channel

The AWGN-2 channel capacity can be obtained by Monte Carlo simulation of Eq. (12). For brevity we omit a plot of it here. The probability of uncoded M-PPM symbol error is given by

$$P_M = 1 - \int_{-\infty}^{\infty} \phi\left(\sqrt{\gamma}(x - \sqrt{\rho})\right) \Phi(x)^{M-1} dx \tag{20}$$

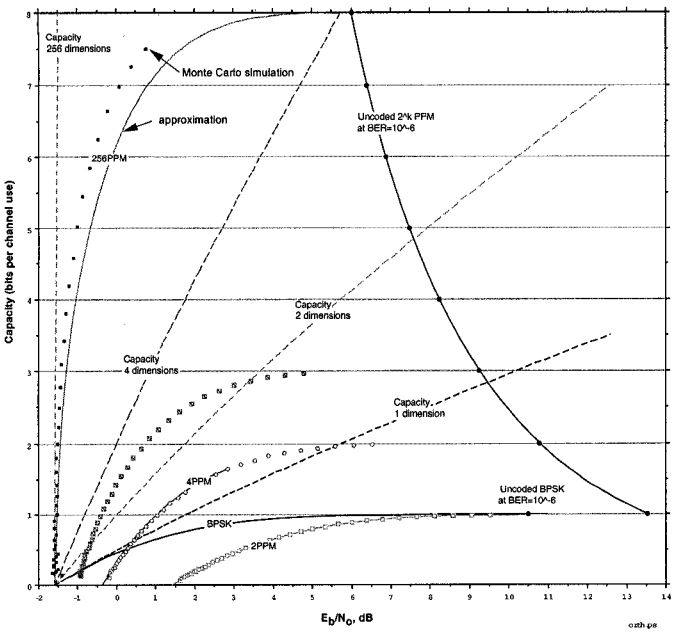

Fig. 2. PPM capacity on AWGN-1 channel, determined from Eq. (8).

Note that when $\gamma \to 1$ and $m_0 \to 0$, the AWGN-2 channel becomes the AWGN-1 channel, and Eq. (20) reduces to Eq. (19).

For M-PPM on an AWGN-2 channel, both the uncoded probability of symbol error and the capacity in Eq. (12) are functions of the parameters $\rho = (m_1 - m_0)^2/\sigma_0^2$ and $\gamma = \sigma_0^2/\sigma_1^2$. This is a statement that the AWGN-2 channel is fully characterized by its SNR and the ratio of the variances.

C. The Webb Channels

We evaluated the M-dimensional expectations in (8), (12), and (18) accurately via Monte Carlo simulation. Some results are plotted in Fig. 3 for the AWGN-1 and Webb-2 channels for different PPM orders M. Along each Webb-2 curve, the two independent variables held constant are $\Delta = 60.8$ and $\rho\gamma/(1-\gamma) = 17.6$, which correspond to a representative optical APD problem with $\eta n_s = 38$ detected signal photons per PPM word and an excess noise factor $F = 2.16$. The results show that the capacity of M-ary orthogonal signaling on the Webb channel exhibits the same brick-wall Shannon limit $(M \ln 2)/(M-1)$ as on the AWGN channel (≈ -1.59 dB for large M). (When translated from an M-ary orthogonal to an M-ary simplex signal set, each curve would have a brick wall at -1.159 dB.) A comparison of hard- and soft-output Webb-2 channels is shown in Fig 4, where a 3dB gain is seen for the soft channel.

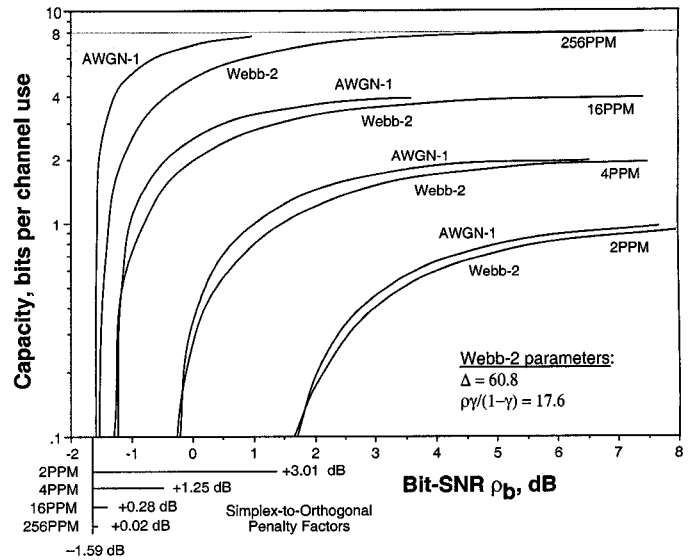

Fig. 3. Capacity of AWGN-1 and Webb-2 channels for different PPM sizes.

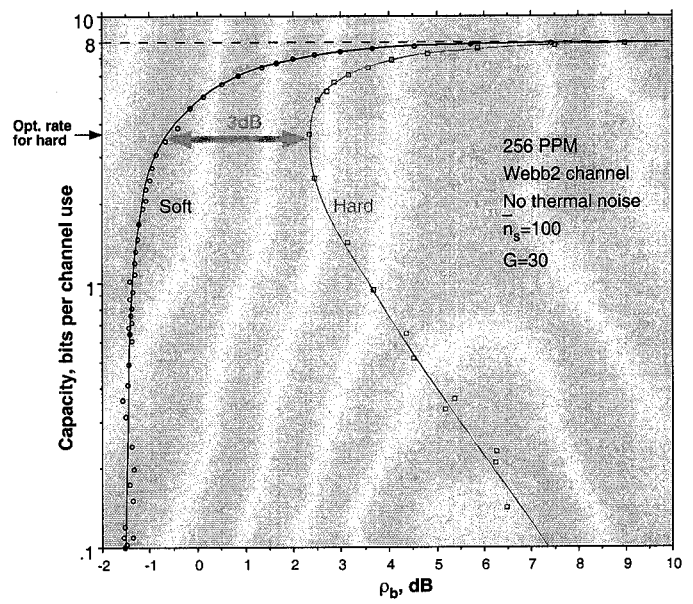

Fig. 4. Capacity of 256-PPM on the hard- and soft-output Webb-2 channels.

IV. COMPARISON OF CAPACITY RESULTS WITH ACTUAL CODE PERFORMANCE

Fig. 5 shows the performance of Reed-Solomon (RS) codes on GF(2^k) applied to 2^k-PPM for $P_b = 10^{-6}$. For each curve the alphabet size is fixed and therefore the Reed-Solomon codeword size is fixed at $(2^k - 1)$ k-bit symbols. The curves are obtained by varying the code rate within each RS code family. For these curves, the RS decoder is assumed to correct only errors (i.e., no erasures), and the uncoded symbol error probability is

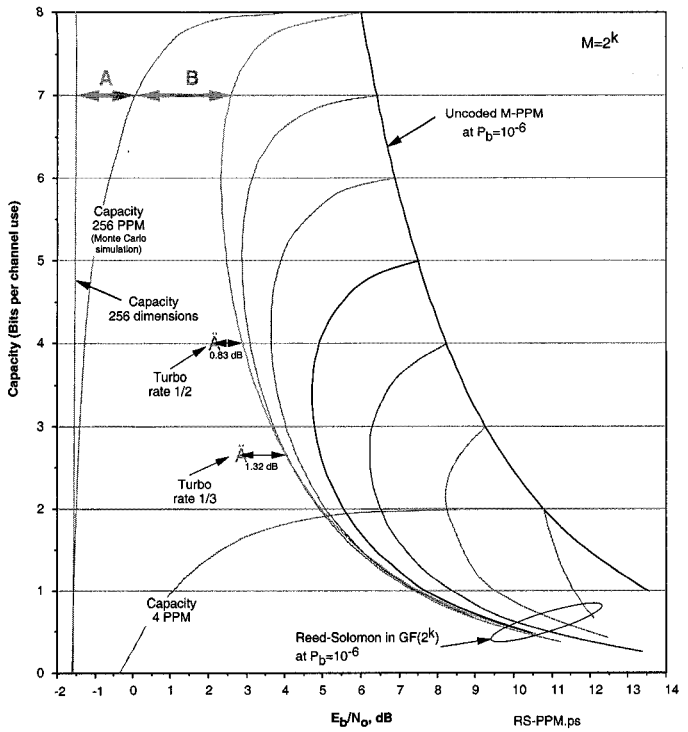

Fig. 5. RS code performance compared to PPM capacity.

given by Eq. (19) with $M = 2^k$. As an example, the performance of the (255,223) RS code, with code rate approximately 7/8, is plotted at approximately 7 bits per channel use on the 8-bit RS curve in Fig. 5. This code requires 2.6 dB for $P_b = 10^{-6}$, and is only 1.8 dB worse than the capacity limit achievable by arbitrary codes of the same rate for 256-PPM (see gap marked with "B" in Fig. 5). The additional gap, marked as "A", is due to constraining the 256-dimensional signal set to be orthogonal. Note that the comparison between the performance of RS codes and the two capacity limits does not account for the fact that the RS decoder uses hard quantized inputs while both capacity limits are computed for unconstrained channel output. This limitation must account for some portion of the non-optimality of RS codes. Another interesting observation from Fig. 5 is that RS codes appear to be optimum approximately at rate 3/4 for all alphabet sizes. Lower-rate RS codes have progressively worse performance.

Some results are available on simple binary turbo codes of rate 1/2 and 1/3 compared to RS codes of the same rate.[1] (See also [4].) These results indicate that, while these binary turbo codes do outperform RS codes of the same rate, there still remains a gap of several dB to the capacity limit.

[1] "Data Compression and Channel Coding", X2000 Report, JPL, Sept. 15, 1997.

V. CONCLUSIONS

This paper has analyzed channel models that can be used to approximate an APD-detected optical communication channel. We were able to define a suitable bit-normalized SNR parameter ρ_b such that all of these channels with soft outputs yield brick-wall thresholds on the minimum acceptable value of ρ_b above which reliable communication is theoretically possible and below which it is not possible. Furthermore, under all of these models with soft channel outputs, the bit-SNR thresholds for different values of M differ from each other by the "simplex-to-orthogonal penalty" $\frac{M-1}{M}$. Under both the AWGN-2 and Webb-2 models, the gap between the capacities of hard- and soft-output channels is about 3 dB at the code rate giving the optimum hard-output bit-SNR. On the hard-output channels, there is an optimum M beyond which capacity is diminished because much of the small incremental information available from each slot is destroyed when all of that information must be summarized as a single decision among an increasing number of candidate slots. This contrasts sharply with the results for soft decisions, for which larger M gives uniformly better capacity under each model.

References

[1] S. Butman and M.J. Klass, "Capacity of noncoherent channels", JPL Technical Report 32-1526 (DSN Progress Report), Vol. XVIII, pp. 85-93, Sept. 1973.

[2] F.M. Davidson and X. Sun. "Gaussian approximation versus nearly exact performance analysis of optical communication systems with PPM signaling and APD receivers". *IEEE Trans. Commun.*, 36(11):1185-1192, November 1988.

[3] R.G. Gallager, *"Information Theory and Reliable Communications"*, New York: Wiley, 1968

[4] J.Hamkins and M. Srinivasan, "Turbo codes for APD-detected PPM", *Allerton Conference*, Oct. 1998

[5] S.J. MacMullan and O.M. Collins, "The capacity of orthogonal and bi-orthogonal codes on the Gaussian Channel", *IEEE Trans on Information Theory*, Vol. 44. No.3, May 1998.

[6] PPM performance for Reed-Solomon decoding over an optical-RF relay link. Divsalar, D. ; Gagliardi, R. M. ; Yuen, J. H. Author Affiliation: JPL, Pasadena, Calif, USA Source: IEEE Trans Commun v COM-32 n 3 Mar 1984 p 302-305

[7] J.Hamkins, "The capacity of APD-detected PPM", The Telecommunications and Mission Operations Progress Report, August 15, 1999.

[8] J. T. K. Tang and K. B. Letaief, "The Use of WMC Distribution for Performance Evaluation of APD Optical Communication Systems", *IEEE Trans Commun*, vol. 46, no. 2, Feb., 1998, pp. 279-285.

[9] V. Vilnrotter, M. Simon, and M. Srinivasan, "Maximum Likelihood Detection of PPM Signals Governed by an Arbitrary Point Process Plus Additive Gaussian Noise", JPL Publication, 98-7, Apr. 1998.

[10] P. P. Webb, R. J. McIntyre, J. Conradi, "Properties of Avalanche Photodiodes", *RCA Review*, vol. 35, Jun. 1974, pp. 234-278.